

Appendix A: Possible line emission contamination from the telescope side lobes

In order to determine whether or not the emission from the bright Orion BN/KL region contributes to our detected signal, we compared the 1 mm spectrum of the Orion Bar with that of Orion BN/KL (located at $\sim 2'$ north of the Bar, e.g. Tercero et al. 2010). Figure A.1 shows several H_2CS and CH_3OH lines observed towards the Bar (black histogram) and Orion BN/KL (red histogram; see Tercero et al. 2010, 2015). We note that the amplitude of Orion BN/KL spectra are divided by a given value to match the line intensities from the Bar. This comparison shows that while the line emission from the Orion Bar peaks at $v_{\text{LSR}} \approx 10.7 \text{ km s}^{-1}$, and can be fully attributed to gas in the PDR (Goicoechea et al. 2016), the blue-shifted shoulder emission seen in some lines at $\sim 8 \text{ km s}^{-1}$ is likely produced by the intense emission from Orion BN/KL, and perhaps by the extended Orion cloud component (for the low-excitation lines). This emission is detected through the telescope extended side lobes and results in a blue-shifted emission shoulder in some spectra towards the Bar. For the IRAM 30 m telescope, the contribution of the secondary lobes increases with frequency (Greve et al. 1998). Given the specific emission velocity and narrow line widths of the emission from the Bar, and the fact that this effect is stronger at $\sim 1 \text{ mm}$, we conclude that our line assignments and line intensity extraction in the PDR is correct.

Appendix B: Identified lines of complex organic molecules

A summary of the main line spectroscopic parameters is presented in Tables B.1-B.11. Line frequency (in MHz), energy of the upper level of each transition (E_u/k in K), Einstein coefficient for spontaneous emission (A_{ul} in s^{-1}), intrinsic line strength (S_{ul}), and the level degeneracy (g_u) from MADEX spectral catalogue, and JPL and CDMS molecular databases are shown. The velocity-integrated line intensity ($\int T_{\text{MB}} dv$ in mK km s^{-1}), LSR velocity (v_{LSR} in km s^{-1}), FWHM line width (Δv in km s^{-1}), and the line peak temperature (T_{MB} in mK) were obtained from Gaussian fits. Parentheses indicate the uncertainty. When two or more transitions were found to overlap, the total profile was fitted. Fully overlapping transitions are marked with connecting symbols in the tables.

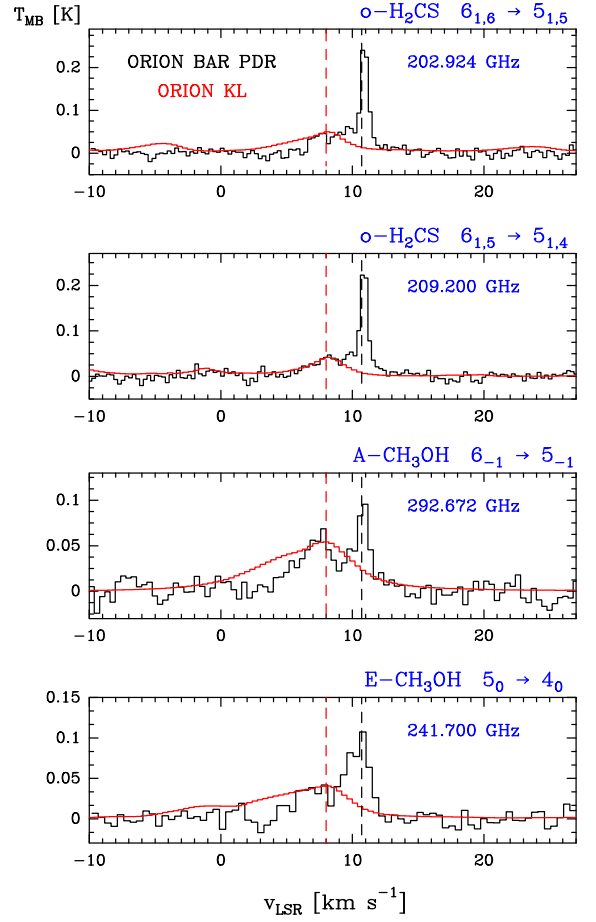


Fig. A.1. Orion Bar spectra (black) at different frequencies in the 1 mm range. For each line, the spectrum towards Orion BN/KL is also shown in red (Tercero et al. 2010, 2015). The CH_3OH spectra towards Orion BN/KL have been divided by ~ 400 , and the H_2CS spectra by ~ 200 . The black and red dashed lines indicate the LSR velocity of the Orion Bar PDR (10.7 km s^{-1}) and Orion extended ridge and/or south hot core ($\sim 8 \text{ km s}^{-1}$, see e.g. Cernicharo et al. 2016), respectively.

Table B.1. Line parameters of HCO.

Transition (N_{K_a, K_c}, J, F) _u → (N_{K_a, K_c}, J, F) _l	Frequency [MHz]	E_u/k [K]	A_{ul} [s ⁻¹]	S_{ul}	g_u	$\int T_{MB} dv$ [mK km s ⁻¹]	v_{LSR} [km s ⁻¹]	Δv [km s ⁻¹]	T_{MB} [mK]	S/N
1 _{0,1} , 3/2, 2 → 0 _{0,0} , 1/2, 1	86670.760 ^F	4.2	4.68 × 10 ⁻⁶	1.66	5	497(12)	10.5(<0.1)	3.1(0.1)	149	52
1 _{0,1} , 3/2, 1 → 0 _{0,0} , 1/2, 0	86708.360 ^F	4.2	4.59 × 10 ⁻⁶	0.98	3	286(7)	10.5(<0.1)	2.8(0.1)	95	33
1 _{0,1} , 1/2, 1 → 0 _{0,0} , 1/2, 1	86777.460 ^F	4.2	4.60 × 10 ⁻⁶	0.98	3	294(7)	10.5(<0.1)	3.0(0.1)	92	32
1 _{0,1} , 1/2, 0 → 0 _{0,0} , 1/2, 1	86805.780 ^F	4.2	4.71 × 10 ⁻⁶	0.33	1	75(6)	10.5(0.1)	2.3(0.2)	31	10
2 _{0,2} , 5/2, 3 → 1 _{0,1} , 3/2, 2	173377.377 ^W	12.5	4.50 × 10 ⁻⁵	2.80	7	683(86)	—	—	—	8
2 _{0,2} , 5/2, 2 → 1 _{0,1} , 3/2, 1	173406.082 ^W	12.5	4.42 × 10 ⁻⁵	1.96	5	346(70)	—	—	—	6
2 _{0,2} , 3/2, 2 → 1 _{0,1} , 1/2, 1	173443.065 ^W	12.5	3.38 × 10 ⁻⁵	1.50	5	409(94)	—	—	—	5
2 _{0,2} , 3/2, 1 → 1 _{0,1} , 1/2, 0	173474.400 ^W	12.5	2.50 × 10 ⁻⁵	0.66	3	185(79)	—	—	—	4
3 _{0,3} , 7/2, 4 → 2 _{0,2} , 5/2, 3	260060.329 ^F	25.0	1.63 × 10 ⁻⁴	3.85	9	576(15)	10.5(<0.1)	2.0(0.1)	275	23
3 _{0,3} , 7/2, 3 → 2 _{0,2} , 5/2, 2	260082.192 ^F	25.0	1.60 × 10 ⁻⁴	2.95	7	446(15)	10.5(<0.1)	2.0(0.1)	209	16
3 _{0,3} , 5/2, 3 → 2 _{0,2} , 3/2, 2	260133.586 ^F	25.0	1.45 × 10 ⁻⁴	2.67	7	347(17)	10.6(<0.1)	1.7(0.4)	195	15
3 _{0,3} , 5/2, 2 → 2 _{0,2} , 3/2, 1	260155.769 ^W	25.0	1.37 × 10 ⁻⁴	1.80	5	382(25)	—	—	—	19
4 _{0,4} , 9/2, 5 → 3 _{0,3} , 7/2, 4	346708.493 ^F	41.6	3.99 × 10 ⁻⁴	4.88	11	437(38)	10.6(0.1)	2.6(0.3)	156	7
4 _{0,4} , 9/2, 4 → 3 _{0,3} , 7/2, 3	346725.172 ^F	41.6	3.95 × 10 ⁻⁴	3.95	9	308(36)	10.6(0.1)	2.0(0.3)	142	7
4 _{0,4} , 7/2, 4 → 3 _{0,3} , 5/2, 3	346787.898 ^F	41.6	3.76 × 10 ⁻⁴	3.76	9	362(41)	10.5(0.2)	3.0(0.5)	112	6
4 _{0,4} , 7/2, 3 → 3 _{0,3} , 5/2, 2	346804.597 ^F	41.6	3.67 × 10 ⁻⁴	2.85	7	223(29)	10.6(0.1)	1.6(0.3)	127	7

Notes. Frequencies, E_u/k , A_{ul} , S_{ul} , and g_u from JPL catalogue. **Labels:** ^F Detected with FTS backend. ^W The lines detected with WILMA backend just give information about the integrated line intensity (see Cuadrado et al. 2015). * Symmetry (ortho-para or E-A).

Table B.2. Line parameters of H₂CO.

Transition (J_{K_a, K_c}) _u → (J_{K_a, K_c}) _l	Sym.*	Frequency [MHz]	E_u/k [K]	A_{ul} [s ⁻¹]	S_{ul}	g_u	$\int T_{MB} dv$ [mK km s ⁻¹]	v_{LSR} [km s ⁻¹]	Δv [km s ⁻¹]	T_{MB} [mK]	S/N
2 _{1,2} → 1 _{1,1}	<i>ortho</i>	140839.516 ^W	6.8	5.30 × 10 ⁻⁵	1.5	5	13488(28)	—	—	—	423
2 _{0,2} → 1 _{0,1}	<i>para</i>	145602.951 ^W	10.5	7.80 × 10 ⁻⁵	2.0	5	5611(67)	—	—	—	95
2 _{1,1} → 1 _{1,0}	<i>ortho</i>	150498.335 ^W	7.5	6.46 × 10 ⁻⁵	1.5	5	10850(97)	—	—	—	208
3 _{1,3} → 2 _{1,2}	<i>ortho</i>	211211.449 ^F	16.9	2.27 × 10 ⁻⁴	2.7	7	13732(26)	10.6(0.1)	2.3(0.1)	5519	338
3 _{0,3} → 2 _{0,2}	<i>para</i>	218222.187 ^F	21.0	2.81 × 10 ⁻⁴	3.0	7	6567(22)	10.6(0.1)	2.2(0.1)	2771	311
3 _{2,2} → 2 _{2,1}	<i>para</i>	218475.634 ^F	68.1	1.57 × 10 ⁻⁴	1.7	7	2600(9)	10.7(0.1)	2.1(0.1)	1148	175
3 _{2,1} → 2 _{2,0}	<i>para</i>	218760.062 ^F	68.1	1.58 × 10 ⁻⁴	1.7	7	2582(12)	10.7(0.1)	2.1(0.1)	1145	151
3 _{1,2} → 2 _{1,1}	<i>ortho</i>	225697.772 ^F	18.3	2.77 × 10 ⁻⁴	2.7	7	11382(39)	10.6(0.1)	2.4(0.1)	4537	269
4 _{1,4} → 3 _{1,3}	<i>ortho</i>	281526.919 ^F	30.4	5.87 × 10 ⁻⁴	3.8	9	15275(49)	10.5(0.1)	2.4(0.1)	6032	409
4 _{2,3} → 3 _{2,2}	<i>para</i>	291237.765 ^F	82.1	5.20 × 10 ⁻⁴	3.0	9	2870(19)	10.6(0.1)	2.1(0.1)	1266	100
4 _{3,2} → 3 _{3,1}	<i>ortho</i>	291380.441 ^F	125.8	3.04 × 10 ⁻⁴	1.8	9	3815(19)	10.6(0.1)	2.0(0.1)	1755	138
4 _{3,1} → 3 _{3,0}	<i>ortho</i>	291384.360 ^F	125.8	3.04 × 10 ⁻⁴	1.8	9	4282(21)	10.7(0.1)	2.3(0.1)	1744	138
4 _{2,2} → 3 _{2,1}	<i>para</i>	291948.066 ^F	82.1	5.24 × 10 ⁻⁴	3.0	9	2863(19)	10.6(0.1)	2.2(0.1)	1244	101
4 _{1,3} → 3 _{1,2}	<i>ortho</i>	300836.630 ^F	32.7	7.17 × 10 ⁻⁴	3.8	9	9897(49)	10.7(0.1)	2.5(0.1)	3668	135
5 _{1,5} → 4 _{1,4}	<i>ortho</i>	351768.637 ^F	47.3	1.20 × 10 ⁻³	4.8	11	8551(88)	10.7(0.1)	2.4(0.1)	3294	61

Notes. Frequencies, E_u/k , A_{ul} , S_{ul} , and g_u from MADEX code, that fit to all rotational lines reported by Bocquet et al. (1996), Brünken et al. (2003), and Eliet et al. (2012).

Table B.3. Line parameters of H₂¹³CO.

Transition ($J_{K_a, K_c})_u \rightarrow (J_{K_a, K_c})_l$	Sym.*	Frequency [MHz]	E_u/k [K]	A_{ul} [s ⁻¹]	S_{ul}	g_u	$\int T_{MB} dv$ [mK km s ⁻¹]	v_{LSR} [km s ⁻¹]	Δv [km s ⁻¹]	T_{MB} [mK]	S/N
2 _{1,2} → 1 _{1,1}	<i>ortho</i>	137449.954 ^W	6.6	4.92×10^{-5}	1.5	5	298(53)	—	—	—	7
2 _{1,1} → 1 _{1,0}	<i>ortho</i>	146635.669 ^W	7.3	5.98×10^{-5}	1.5	5	73(29)	—	—	—	5
3 _{1,3} → 2 _{1,2}	<i>ortho</i>	206131.619 ^F	16.5	2.11×10^{-4}	2.6	7	251(12)	10.5(0.1)	2.4(0.1)	97	11
3 _{0,3} → 2 _{0,2}	<i>para</i>	212811.190 ^F	20.4	2.61×10^{-4}	3.0	7	84(13)	10.3(0.1)	2.1(0.4)	37	4
3 _{1,2} → 2 _{1,1}	<i>ortho</i>	219908.481 ^F	17.8	2.56×10^{-4}	2.7	7	151(12)	10.7(0.1)	2.0(0.2)	70	7
4 _{1,4} → 3 _{1,3}	<i>ortho</i>	274762.103 ^F	29.7	5.46×10^{-4}	3.8	9	180(16)	10.8(0.1)	2.3(0.3)	74	6
4 _{0,4} → 3 _{0,3}	<i>para</i>	283441.868 ^F	34.0	6.39×10^{-4}	4.0	9	32(13)	10.7(0.2)	0.9(0.5)	33	4
4 _{1,3} → 3 _{1,2}	<i>ortho</i>	293126.495 ^F	31.9	6.63×10^{-4}	3.8	9	140(13)	10.5(0.1)	2.3(0.3)	58	6

Notes. Frequencies, E_u/k , A_{ul} , S_{ul} , and g_u from MADEX code, that fit to all rotational lines reported by Müller et al. (2000).

Table B.4. Line parameters of H₂CS.

Transition ($J_{K_a, K_c})_u \rightarrow (J_{K_a, K_c})_l$	Sym.*	Frequency [MHz]	E_u/k [K]	A_{ul} [s ⁻¹]	S_{ul}	g_u	$\int T_{MB} dv$ [mK km s ⁻¹]	v_{LSR} [km s ⁻¹]	Δv [km s ⁻¹]	T_{MB} [mK]	S/N
3 _{1,3} → 2 _{1,2}	<i>ortho</i>	101477.810 ^F	8.1	1.26×10^{-5}	2.67	7	79(8)	10.8(0.1)	1.1(0.1)	68	10
3 _{2,2} → 2 _{2,1}	<i>para</i>	103039.907 ^F	62.6	8.25×10^{-6}	1.67	7	} 53(5)	10.9(0.1)	1.8(0.2)	28	9
3 _{0,3} → 2 _{0,2}	<i>para</i>	103040.452 ^F	9.9	1.48×10^{-5}	3.00	7		19(7)	10.5(0.3)	1.5(1.3)	10
3 _{2,1} → 2 _{2,0}	<i>para</i>	103051.847 ^F	62.6	8.25×10^{-6}	1.67	7	85(5)	10.7(<0.1)	1.3(0.1)	59	14
3 _{1,2} → 2 _{1,1}	<i>ortho</i>	104617.040 ^F	8.4	1.38×10^{-5}	2.67	7	182(18)	—	—	—	2
4 _{0,4} → 3 _{0,3}	<i>para</i>	137371.210 ^W	16.5	3.65×10^{-5}	4.00	9	149(22)	—	—	—	4
4 _{1,3} → 3 _{1,2}	<i>ortho</i>	139483.682 ^W	15.1	3.58×10^{-5}	3.75	9	229(35)	—	—	—	10
5 _{1,5} → 4 _{1,4}	<i>ortho</i>	169114.079 ^W	22.7	6.68×10^{-5}	4.80	11	1447(217)	—	—	—	9
5 _{0,5} → 4 _{0,4}	<i>para</i>	171688.117 ^W	24.7	7.28×10^{-5}	5.00	11	300(106)	—	—	—	3
5 _{1,4} → 4 _{1,3}	<i>ortho</i>	174345.223 ^W	23.5	7.32×10^{-5}	4.80	11	206(10)	10.9(<0.1)	0.8(0.1)	245	18
6 _{0,6} → 5 _{0,5}	<i>para</i>	205987.858 ^F	34.6	1.28×10^{-4}	6.00	13	75(7)	10.9(<0.1)	0.7(0.1)	104	10
6 _{3,4} → 5 _{3,3}	<i>ortho</i>	206052.602 ^F	138.3	9.59×10^{-5}	4.50	13	} 76(14)	10.9(0.1)	1.3(0.4)	55	5
6 _{3,3} → 5 _{3,2}	<i>ortho</i>	206052.602 ^F	138.3	9.59×10^{-5}	4.50	13		48(7)	10.9(0.1)	1.0(0.1)	47
6 _{2,4} → 5 _{2,3}	<i>para</i>	206158.602 ^F	87.3	1.14×10^{-4}	5.33	13	190(9)	10.9(<0.1)	0.8(0.1)	231	17
6 _{1,5} → 5 _{1,4}	<i>ortho</i>	209200.620 ^F	33.5	1.30×10^{-4}	5.83	13	105(14)	10.9(<0.1)	0.5(0.1)	185	7
7 _{1,7} → 6 _{1,6}	<i>ortho</i>	236727.020 ^F	43.8	1.92×10^{-4}	6.86	15	107(13)	10.8(<0.1)	0.9(0.1)	116	8
7 _{0,7} → 6 _{0,6}	<i>para</i>	240266.872 ^F	46.1	2.05×10^{-4}	7.00	15	24(6)	10.8(0.1)	0.3(0.2)	76	3
7 _{2,6} → 6 _{2,5}	<i>para</i>	240382.051 ^F	98.8	1.88×10^{-4}	6.43	15	} 122(14)	10.5(0.1)	1.6(0.2)	72	6
7 _{3,5} → 6 _{3,4}	<i>ortho</i>	240393.037 ^F	149.8	1.68×10^{-4}	5.71	15		62(11)	10.7(0.1)	1.5(0.2)	54
7 _{3,4} → 6 _{3,3}	<i>ortho</i>	240393.762 ^F	149.8	1.68×10^{-4}	5.71	15					
7 _{2,5} → 6 _{2,4}	<i>para</i>	240549.066 ^F	98.8	1.89×10^{-4}	6.43	15					

Table B.4. continued.

Transition $(J_{K_a, K_c})_u \rightarrow (J_{K_a, K_c})_l$	Sym.*	Frequency [MHz]	E_u/k [K]	A_{ul} [s ⁻¹]	S_{ul}	g_u	$\int T_{MB} dv$ [mK km s ⁻¹]	v_{LSR} [km s ⁻¹]	Δv [km s ⁻¹]	T_{MB} [mK]	S/N
$7_{1,6} \rightarrow 6_{1,5}$	<i>ortho</i>	244048.504 ^F	45.2	2.10×10^{-4}	6.86	15	185(11)	10.9(<0.1)	0.8(0.1)	260	14
$8_{1,8} \rightarrow 7_{1,7}$	<i>ortho</i>	270521.931 ^F	56.8	2.90×10^{-4}	7.88	17	128(16)	10.8(0.1)	0.9(0.2)	139	6
$8_{0,8} \rightarrow 7_{0,7}$	<i>para</i>	274521.931 ^F	59.3	3.08×10^{-4}	8.00	17	60(9)	11.1(0.1)	0.7(0.1)	77	5
$8_{2,6} \rightarrow 7_{2,5}$	<i>para</i>	274953.744 ^F	112.0	2.90×10^{-4}	7.50	17	36(9)	11.0(0.1)	0.9(0.2)	39	3
$8_{1,7} \rightarrow 7_{1,6}$	<i>ortho</i>	278887.661 ^F	58.6	3.18×10^{-4}	7.87	17	195(13)	10.9(<0.1)	0.7(0.1)	245	14
$9_{1,9} \rightarrow 8_{1,8}$	<i>ortho</i>	304307.709 ^F	71.4	4.17×10^{-4}	8.89	19	75(8)	10.7(0.1)	0.7(0.1)	101	5
$10_{1,10} \rightarrow 9_{1,9}$	<i>ortho</i>	338083.195 ^F	87.6	5.77×10^{-4}	9.90	21	108(30)	10.6(0.1)	0.9(0.3)	113	3

Notes. Frequencies, E_u/k , A_{ul} , S_{ul} , and g_u from CDMS catalogue.

Table B.5. Line parameters of HNCO.

Transition $(J_{K_a, K_c})_u \rightarrow (J_{K_a, K_c})_l$	Frequency [MHz]	E_u/k [K]	A_{ul} [s ⁻¹]	S_{ul}	g_u	$\int T_{MB} dv$ [mK km s ⁻¹]	v_{LSR} [km s ⁻¹]	Δv [km s ⁻¹]	T_{MB} [mK]	S/N
$4_{0,4} \rightarrow 3_{0,3}$	87925.237 ^F	10.5	9.03×10^{-6}	4.0	9	49(6)	10.8(0.1)	1.7(0.2)	27	8
$5_{0,5} \rightarrow 4_{0,4}$	109905.749 ^F	15.8	1.80×10^{-5}	5.0	11	110(9)	10.6(0.1)	1.9(0.2)	54	10
$7_{0,7} \rightarrow 6_{0,6}$	153865.086 ^W	29.5	5.08×10^{-5}	7.0	15	125(39)	—	—	—	3
$10_{0,10} \rightarrow 9_{0,9}$	219798.274 ^F	58.0	1.51×10^{-4}	10.0	21	154(16)	10.6(0.2)	3.3(0.4)	44	6
$11_{0,11} \rightarrow 10_{0,10}$	241774.032 ^F	69.6	2.02×10^{-4}	11.0	23	118(21)	10.7(0.1)	1.6(0.3)	69	5
$13_{0,13} \rightarrow 12_{0,12}$	285721.951 ^F	96.0	3.36×10^{-4}	13.0	27	129(26)	10.4(0.3)	2.8(0.7)	43	5

Notes. Frequencies, E_u/k , A_{ul} , S_{ul} , and g_u from CDMS catalogue.

Table B.6. Line parameters of CH₂NH.

Transition $(J_{K_a, K_c})_u \rightarrow (J_{K_a, K_c})_l$	Frequency [MHz]	E_u/k [K]	A_{ul} [s ⁻¹]	S_{ul}	g_u	$\int T_{MB} dv$ [mK km s ⁻¹]	v_{LSR} [km s ⁻¹]	Δv [km s ⁻¹]	T_{MB} [mK]	S/N
$4_{0,4} \rightarrow 3_{1,3}$	105794.062 ^F	30.6	1.62×10^{-5}	5.0	9	55(13)	11.3(0.5)	4.2(1.3)	12	3
$1_{1,1} \rightarrow 0_{0,0}$	225554.609 ^F	10.8	2.79×10^{-4}	3.0	3	120(26)	10.5(0.2)	2.9(0.9)	39	4
$4_{1,4} \rightarrow 3_{1,3}$	245125.866 ^F	37.3	3.85×10^{-4}	11.2	9	106(14)	11.1(0.1)	2.3(0.4)	43	4
$6_{0,6} \rightarrow 5_{1,5}$	251421.265 ^F	64.1	2.73×10^{-4}	9.2	13	72(13)	11.0(0.3)	3.1(0.6)	22	4
$4_{0,4} \rightarrow 3_{0,3}$	254685.137 ^F	30.6	4.60×10^{-4}	12.0	9	314(12)	10.8(0.1)	2.0(0.1)	147	14
$4_{1,3} \rightarrow 3_{1,2}$	266270.024 ^F	39.8	4.93×10^{-4}	11.2	9	117(12)	10.9(0.1)	2.0(0.2)	54	5

Notes. Frequencies, E_u/k , A_{ul} , S_{ul} , and g_u from CDMS catalogue.

Table B.7. Line parameters of H₂CCO.

Transition ($J_{K_a, K_c})_u \rightarrow (J_{K_a, K_c})_l$	Sym.*	Frequency [MHz]	E_u/k [K]	A_{ul} [s ⁻¹]	S_{ul}	g_u	$\int T_{MB} dv$ [mK km s ⁻¹]	v_{LSR} [km s ⁻¹]	Δv [km s ⁻¹]	T_{MB} [mK]	S/N
4 _{2,3} → 3 _{2,2}	<i>para</i>	80820.400 ^F	61.9	4.14 × 10 ⁻⁶	3.0	9	13(9)	10.9(0.7)	1.6(0.7)	8	2
4 _{1,3} → 3 _{1,2}	<i>ortho</i>	81586.239 ^F	8.8	5.33 × 10 ⁻⁶	3.8	9	44(8)	11.0(0.3)	2.5(0.6)	13	4
5 _{1,5} → 4 _{1,4}	<i>ortho</i>	100094.511 ^F	13.5	1.03 × 10 ⁻⁵	4.8	11	61(6)	10.4(0.2)	1.9(0.5)	30	3
5 _{3,3} → 4 _{3,2}	<i>ortho</i>	101002.349 ^F	117.9	7.06 × 10 ⁻⁶	3.2	11	} 25(8)	10.3(0.2)	1.0(0.3)	25	3
5 _{3,2} → 4 _{3,1}	<i>ortho</i>	101002.354 ^F	117.9	7.06 × 10 ⁻⁶	3.2	11					
5 _{2,4} → 4 _{2,3}	<i>para</i>	101024.430 ^F	66.7	9.27 × 10 ⁻⁶	4.2	11	24(6)	10.2(0.2)	1.7(0.8)	15	2
5 _{1,4} → 4 _{1,3}	<i>ortho</i>	101981.442 ^F	13.7	1.09 × 10 ⁻⁵	4.8	11	58(6)	10.9(0.1)	2.3(0.3)	24	7
7 _{1,7} → 6 _{1,6}	<i>ortho</i>	140127.471 ^W	25.9	2.96 × 10 ⁻⁵	6.9	15	107(43)	—	—	—	5
7 _{3,5} → 6 _{3,4}	<i>ortho</i>	141402.460 ^W	130.5	2.54 × 10 ⁻⁵	5.7	15	} 71(32)	—	—	—	4
7 _{3,4} → 6 _{3,3}	<i>ortho</i>	141402.491 ^W	130.5	2.54 × 10 ⁻⁵	5.7	15					
8 _{1,7} → 7 _{1,6}	<i>ortho</i>	163160.893 ^W	34.3	4.74 × 10 ⁻⁵	7.9	17	114(22)	—	—	—	5
11 _{1,11} → 10 _{1,10}	<i>ortho</i>	220177.558 ^F	62.4	1.19 × 10 ⁻⁴	10.9	23	128(13)	10.8(0.1)	2.6(0.3)	47	5
11 _{3,9} → 10 _{3,8}	<i>ortho</i>	222199.879 ^F	167.4	1.14 × 10 ⁻⁴	10.2	23	} 120(13)	10.5(0.1)	1.9(0.5)	59	8
11 _{3,8} → 10 _{3,7}	<i>ortho</i>	222200.199 ^F	167.4	1.14 × 10 ⁻⁴	10.2	23					
11 _{2,10} → 10 _{2,9}	<i>para</i>	222228.629 ^F	116.2	1.20 × 10 ⁻⁴	10.6	23	54(15)	10.7(0.1)	2.0(0.8)	25	4
11 _{1,10} → 10 _{1,9}	<i>ortho</i>	224327.246 ^F	63.6	1.26 × 10 ⁻⁴	10.9	23	125(11)	10.8(0.1)	2.5(0.2)	47	7
12 _{1,12} → 11 _{1,11}	<i>ortho</i>	240185.798 ^F	74.0	1.56 × 10 ⁻⁴	11.9	25	123(19)	10.9(0.2)	2.6(0.6)	45	5
12 _{0,12} → 11 _{0,11}	<i>para</i>	242375.721 ^F	75.6	1.61 × 10 ⁻⁴	12.0	25	38(11)	10.5(0.1)	0.8(0.2)	46	2
12 _{1,11} → 11 _{1,10}	<i>ortho</i>	244712.254 ^F	75.4	1.64 × 10 ⁻⁴	11.9	25	123(13)	10.8(0.1)	1.7(0.1)	69	5
13 _{1,13} → 12 _{1,12}	<i>ortho</i>	260191.993 ^W	86.5	1.99 × 10 ⁻⁴	12.9	27	100(19)	—	—	—	7
13 _{0,13} → 12 _{0,12}	<i>para</i>	262548.202 ^F	88.2	2.05 × 10 ⁻⁴	13.0	27	35(9)	10.8(0.1)	1.2(0.2)	28	3
13 _{3,11} → 12 _{3,10}	<i>ortho</i>	262596.638 ^F	191.6	1.94 × 10 ⁻⁴	12.3	27	} 108(17)	10.7(0.1)	2.1(0.3)	46	5
13 _{3,10} → 12 _{3,9}	<i>ortho</i>	262597.384 ^F	191.6	1.94 × 10 ⁻⁴	12.3	27					
13 _{2,12} → 12 _{2,11}	<i>para</i>	262618.994 ^F	140.4	2.00 × 10 ⁻⁴	12.7	27	43(9)	10.7(0.2)	1.5(0.2)	27	3
13 _{2,11} → 12 _{2,10}	<i>para</i>	262760.857 ^F	140.5	2.01 × 10 ⁻⁴	12.7	27	38(15)	10.3(0.3)	1.8(0.8)	20	3
13 _{1,12} → 12 _{1,11}	<i>ortho</i>	265095.061 ^F	88.1	2.10 × 10 ⁻⁴	13.0	27	99(10)	10.7(0.1)	1.5(0.1)	63	6
14 _{1,14} → 13 _{1,13}	<i>ortho</i>	280195.979 ^F	99.9	2.49 × 10 ⁻⁴	13.9	29	128(13)	10.6(0.1)	2.0(0.2)	61	6
14 _{0,14} → 13 _{0,13}	<i>para</i>	282714.584 ^F	101.8	2.57 × 10 ⁻⁴	14.0	29	33(15)	10.8(0.3)	1.0(0.3)	31	3
14 _{3,12} → 13 _{3,11}	<i>ortho</i>	282794.399 ^F	205.2	2.45 × 10 ⁻⁴	13.4	29	} 131(15)	10.5(0.1)	2.0(0.2)	62	6
14 _{3,11} → 13 _{3,10}	<i>ortho</i>	282795.485 ^F	205.2	2.45 × 10 ⁻⁴	13.4	29					
14 _{2,13} → 13 _{2,12}	<i>para</i>	282811.466 ^F	154.0	2.52 × 10 ⁻⁴	13.7	29	39(13)	10.5(0.1)	0.9(0.3)	45	4
14 _{2,12} → 13 _{2,11}	<i>para</i>	282988.739 ^F	154.0	2.52 × 10 ⁻⁴	13.7	29	34(7)	10.7(0.1)	1.0(0.2)	34	4
14 _{1,13} → 13 _{1,12}	<i>ortho</i>	285475.477 ^F	101.8	2.63 × 10 ⁻⁴	13.9	29	107(18)	10.5(0.2)	1.8(0.3)	54	4
15 _{1,15} → 14 _{1,14}	<i>ortho</i>	300197.596 ^F	114.3	3.07 × 10 ⁻⁴	14.9	31	89(39)	10.7(0.4)	1.9(0.5)	44	2
15 _{3,13} → 14 _{3,12}	<i>ortho</i>	302991.695 ^F	219.7	3.04 × 10 ⁻⁴	14.4	31	} 116(28)	11.0(0.3)	2.2(0.4)	49	2
15 _{3,12} → 14 _{3,11}	<i>ortho</i>	302993.234 ^F	219.7	3.04 × 10 ⁻⁴	14.4	31					

Notes. Frequencies, E_u/k , A_{ul} , S_{ul} , and g_u from MADEX code, that fit to all rotational lines reported in the CDMS database.

Table B.8. Line parameters of HC₃N.

Transition	Frequency	E_u/k	A_{ul}	S_{ul}	g_u	$\int T_{MB} dv$	v_{LSR}	Δv	T_{MB}	S/N
$J_u \rightarrow J_l$	[MHz]	[K]	[s ⁻¹]			[mK km s ⁻¹]	[km s ⁻¹]	[km s ⁻¹]	[mK]	
9 → 8	81881.462 ^F	19.6	4.22×10^{-5}	9.0	19	50(19)	10.8(0.2)	2.1(0.6)	23(s)	6
10 → 9	90978.989 ^F	24.0	5.81×10^{-5}	10.0	21	86(11)	10.5(0.2)	2.9(0.4)	28	6
11 → 10	100076.385 ^F	28.8	7.77×10^{-5}	11.0	23	80(14)	10.5(0.2)	1.8(0.3)	42	6
12 → 11	109173.637 ^F	34.1	1.01×10^{-4}	12.0	25	76(8)	10.7(0.1)	2.0(0.2)	37	10
15 → 14	136464.402 ^W	52.4	1.99×10^{-4}	15.0	31	164(59)	—	—	—	3
16 → 15	145560.949 ^W	59.4	2.42×10^{-4}	16.0	33	95(59)	—	—	—	4
17 → 16	154657.288 ^W	66.8	2.91×10^{-4}	17.0	35	162(36)	—	—	—	5
18 → 17	163753.404 ^W	74.7	3.46×10^{-4}	18.0	37	162(20)	—	—	—	8
19 → 18	172849.285 ^W	83.0	4.08×10^{-4}	19.0	39	169(17)	—	—	—	2
23 → 22	209230.199 ^F	120.5	7.27×10^{-4}	23.0	47	54(16)	10.8(0.2)	1.7(0.6)	30	5
24 → 23	218324.709 ^F	131.0	8.26×10^{-4}	24.0	49	16(4)	10.9(0.1)	0.6(0.2)	24	4

Notes. Frequencies, E_u/k , A_{ul} , S_{ul} , and g_u from MADEX code, that fit to all rotational lines reported by de Zafra (1971); Mbosei et al. (2000); Creswell et al. (1977); Chen et al. (1991); Yamada et al. (1995); Thorwirth et al. (2000).

Table B.9. Line parameters of CH₃CN.

Transition	Sym.*	Frequency	E_u/k	A_{ul}	S_{ul}	g_u	$\int T_{MB} dv$	v_{LSR}	Δv	T_{MB}	S/N
$(J_K)_u \rightarrow (J_K)_l$		[MHz]	[K]	[s ⁻¹]			[mK km s ⁻¹]	[km s ⁻¹]	[km s ⁻¹]	[mK]	
5 ₄ → 4 ₄	E	91958.726 ^F	119.5	2.28×10^{-5}	1.8	11	26(13)	12.5(0.5)	2.0(1.0)	13	3
5 ₃ → 4 ₃	A	91971.130 ^F	77.5	4.06×10^{-5}	6.4	22	103(9)	10.2(0.2)	4.0(0.4)	24	6
5 ₂ → 4 ₂	E	91979.993 ^F	33.8	5.33×10^{-5}	4.2	11	84(16)	10.6(0.3)	3.0(0.7)	26	6
5 ₁ → 4 ₁	E	91985.313 ^F	12.4	6.09×10^{-5}	4.8	11	114(12)	10.5(0.1)	2.6(0.4)	40	9
5 ₀ → 4 ₀	A	91987.087 ^F	13.2	6.35×10^{-5}	5.0	11	138(13)	10.9(0.1)	2.8(0.4)	46	11
6 ₃ → 5 ₃	A	110364.353 ^F	82.8	8.35×10^{-5}	9.0	26	151(11)	10.8(0.1)	2.7(0.2)	53	8
6 ₂ → 5 ₂	E	110374.988 ^F	39.1	9.89×10^{-5}	5.3	13	87(10)	10.7(0.1)	2.0(0.3)	40	7
6 ₁ → 5 ₁	E	110381.371 ^F	17.7	1.08×10^{-4}	5.8	13	144(10)	10.8(0.1)	2.1(0.2)	65	10
6 ₀ → 5 ₀	A	110383.499 ^F	18.5	1.11×10^{-4}	6.0	13	137(10)	10.8(0.1)	2.1(0.2)	62	11
7 ₄ → 6 ₄	E	128739.669 ^W	131.0	1.20×10^{-4}	4.7	15	75(49)	—	—	—	2
7 ₃ → 6 ₃	A	128757.029 ^W	89.0	1.46×10^{-4}	11.4	30	181(59)	—	—	—	3
7 ₂ → 6 ₂	E	128769.435 ^W	45.3	1.64×10^{-4}	6.4	15	112(62)	—	—	—	4
7 ₁ → 6 ₁	E	128776.880 ^W	23.8	1.75×10^{-4}	6.8	15	} 425(59)	—	—	—	6
7 ₀ → 6 ₀	A	128779.363 ^W	24.7	1.79×10^{-4}	7.0	15					
8 ₃ → 7 ₃	A	147149.068 ^W	96.1	2.31×10^{-4}	13.8	34	149(31)	—	—	—	4
8 ₂ → 7 ₂	E	147163.243 ^W	52.3	2.52×10^{-4}	7.5	17	98(33)	—	—	—	2
8 ₁ → 7 ₁	E	147171.751 ^W	30.9	2.65×10^{-4}	7.9	17	} 385(41)	—	—	—	8
8 ₀ → 7 ₀	A	147174.587 ^W	31.8	2.69×10^{-4}	8.0	17					
9 ₄ → 8 ₄	E	165518.064 ^W	146.0	3.09×10^{-4}	7.2	19	85(23)	—	—	—	3
9 ₃ → 8 ₃	A	165540.376 ^W	104.0	3.43×10^{-4}	16.0	38	177(20)	—	—	—	9

Table B.9. continued

Transition (J_K) _u → (J_K) _l	Sym.*	Frequency [MHz]	E_u/k [K]	A_{ul} [s ⁻¹]	S_{ul}	g_u	$\int T_{MB} dv$ [mK km s ⁻¹]	v_{LSR} [km s ⁻¹]	Δv [km s ⁻¹]	T_{MB} [mK]	S/N
9 ₂ → 8 ₂	E	165556.321 ^W	60.3	3.66×10^{-4}	8.6	19	108(19)	—	—	—	7
9 ₁ → 8 ₁	E	165565.890 ^W	38.8	3.81×10^{-4}	8.9	19	} 419(24)	—	—	—	14
9 ₀ → 8 ₀	A	165569.080 ^W	39.7	3.86×10^{-4}	9.0	19		—	—	—	—
11 ₃ → 10 ₃	A	202320.442 ^F	122.6	6.58×10^{-4}	20.3	46	140(11)	10.7(0.1)	2.0(0.2)	64	8
11 ₂ → 10 ₂	E	202339.920 ^F	78.8	6.87×10^{-4}	10.6	23	78(9)	10.7(0.1)	1.5(0.2)	49	6
11 ₁ → 10 ₁	E	202351.610 ^F	57.4	7.05×10^{-4}	10.9	23	103(13)	10.7(0.2)	2.9(0.4)	33	5
11 ₀ → 10 ₀	A	202355.507 ^F	58.3	7.11×10^{-4}	11.0	23	135(11)	10.7(0.1)	2.3(0.2)	55	7
12 ₄ → 11 ₄	E	220679.287 ^F	175.1	8.22×10^{-4}	10.7	25	44(12)	10.9(0.3)	1.8(0.5)	23	4
12 ₃ → 11 ₃	A	220709.016 ^F	133.2	8.68×10^{-4}	22.5	50	100(15)	10.7(0.1)	1.8(0.4)	52	8
12 ₂ → 11 ₂	E	220730.259 ^F	89.4	9.00×10^{-4}	11.7	25	61(15)	10.6(0.3)	1.7(0.0)	34	6
12 ₁ → 11 ₁	E	220743.009 ^F	68.0	9.20×10^{-4}	11.9	25	122(15)	10.4(0.1)	1.7(0.2)	72	11
12 ₀ → 11 ₀	A	220747.259 ^F	68.9	9.26×10^{-4}	12.0	25	69(15)	10.9(0.2)	1.7(0.3)	38	6
13 ₃ → 12 ₃	A	239096.495 ^F	144.6	1.12×10^{-3}	24.6	54	94(16)	10.8(0.1)	1.9(0.5)	46	7
13 ₂ → 12 ₂	E	239119.503 ^F	100.9	1.15×10^{-3}	12.7	27	20(11)	10.6(0.3)	1.0(0.8)	19	3
13 ₀ → 12 ₀	A	239137.914 ^F	80.3	1.18×10^{-3}	13.0	27	52(9)	10.5(0.2)	1.3(0.4)	23	3
14 ₄ → 13 ₄	E	257448.128 ^F	199.0	1.36×10^{-3}	12.9	29	29(10)	10.6(0.3)	1.5(0.6)	19	3
14 ₃ → 13 ₃	A	257482.790 ^F	157.0	1.41×10^{-3}	26.7	58	57(17)	10.6(0.2)	1.5(0.3)	36	5
14 ₂ → 13 ₂	E	257507.560 ^F	113.3	1.45×10^{-3}	13.7	29	55(10)	10.7(0.1)	1.3(0.3)	40	6
14 ₁ → 13 ₁	E	257522.425 ^F	91.8	1.47×10^{-3}	13.9	29	53(11)	10.8(0.3)	2.0(0.5)	24	4
14 ₀ → 13 ₀	A	257527.381 ^F	92.7	1.48×10^{-3}	14.0	29	42(8)	10.9(0.1)	1.0(0.2)	38	5
15 ₃ → 14 ₃	A	275867.809 ^F	170.2	1.75×10^{-3}	28.8	62	61(14)	10.5(0.2)	1.5(0.4)	38	4
15 ₂ → 14 ₂	E	275894.339 ^F	126.5	1.79×10^{-3}	14.7	31	31(9)	10.3(0.1)	0.7(0.3)	40	2
15 ₁ → 14 ₁	E	275910.261 ^F	105.1	1.81×10^{-3}	14.9	31	30(12)	10.7(0.2)	0.7(0.2)	40	2
16 ₃ → 15 ₃	A	294251.460 ^F	184.4	2.14×10^{-3}	30.9	66	55(13)	10.1(0.2)	1.2(0.2)	43	4
16 ₂ → 15 ₂	E	294279.748 ^F	140.6	2.18×10^{-3}	15.7	33	33(15)	10.4(0.2)	0.9(0.3)	34	4
16 ₁ → 15 ₁	E	294296.726 ^F	119.2	2.21×10^{-3}	15.9	33	34(9)	10.2(0.1)	1.0(0.2)	32	4
16 ₀ → 15 ₀	A	294302.386 ^F	120.1	2.22×10^{-3}	16.0	33	27(9)	10.9(0.2)	0.8(0.2)	32	2

Notes. Frequencies, E_u/k , A_{ul} , S_{ul} , and g_u from MADEX code, that fit to all rotational lines reported by Kukolich et al. (1973); Boucher et al. (1977); Kukolich (1982); Pavone et al. (1990); Cazzoli & Puzzarini (2006); Šimečková et al. (2004); Müller et al. (2009).

Table B.10. Line parameters of CH₃OH.

Transition ($J_K)_u \rightarrow (J_K)_l$	Sym.*	Frequency [MHz]	E_u/k [K]	A_{ul} [s ⁻¹]	S_{ul}	g_u	$\int T_{MB} dv$ [mK km s ⁻¹]	v_{LSR} [km s ⁻¹]	Δv [km s ⁻¹]	T_{MB} [mK]	S/N
5 ₋₁ → 4 ₀	E	84521.172 ^F	32.5	1.97 × 10 ⁻⁶	1.5	11	149(8)	10.6(0.1)	1.6(0.1)	86	18
8 ₀ → 7 ₁	A	95169.391 ^F	83.5	2.13 × 10 ⁻⁶	1.8	17	59(6)	10.4(0.1)	1.5(0.1)	54	14
2 ₁ → 1 ₁	A	95914.310 ^F	21.4	2.49 × 10 ⁻⁶	1.5	5	28(12)	10.8(0.3)	1.7(0.7)	15	2
2 ₋₁ → 1 ₋₁	E	96739.358 ^F	4.6	2.56 × 10 ⁻⁶	1.5	5	107(9)	10.7(0.1)	1.5(0.1)	67	9
2 ₀ → 1 ₀	A	96741.371 ^F	7.0	3.41 × 10 ⁻⁶	2.0	5	206(9)	10.8(0.1)	1.7(0.2)	114	16
2 ₀ → 1 ₀	E	96744.545 ^F	12.2	3.41 × 10 ⁻⁶	2.0	5	95(12)	10.7(0.1)	1.9(0.3)	44	6
2 ₁ → 1 ₁	E	96755.501 ^F	20.1	2.62 × 10 ⁻⁶	1.5	5	66(13)	10.8(0.2)	2.0(0.5)	27	4
2 ₋₁ → 1 ₋₁	A	97582.798 ^F	21.6	2.63 × 10 ⁻⁶	1.5	5	32(12)	10.5(0.2)	1.7(0.6)	18	4
3 ₁ → 4 ₀	A	107013.831 ^F	28.3	3.07 × 10 ⁻⁶	0.7	7	30(12)	9.7(0.4)	2.2(0.2)	13	3
0 ₀ → 1 ₋₁	E	108893.945 ^F	5.2	1.47 × 10 ⁻⁵	0.5	1	45(6)	10.7(0.1)	1.6(0.2)	26	7
6 ₋₁ → 5 ₀	E	132890.759 ^W	46.4	7.75 × 10 ⁻⁶	1.8	13	191(31)	—	—	—	5
3 ₁ → 2 ₁	A	143865.795 ^W	28.3	1.07 × 10 ⁻⁵	2.7	7	74(28)	—	—	—	3
3 ₋₁ → 2 ₋₁	E	145097.435 ^W	11.6	1.10 × 10 ⁻⁵	2.7	7	269(28)	—	—	—	10
3 ₀ → 2 ₀	A	145103.185 ^W	13.9	1.23 × 10 ⁻⁵	3.0	7	384(83)	—	—	—	12
3 ₋₂ → 2 ₋₂	A	145124.332 ^W	51.6	6.89 × 10 ⁻⁶	1.7	7					
3 ₂ → 2 ₂	E	145126.191 ^W	28.3	6.77 × 10 ⁻⁶	1.7	7	} 103(23)	—	—	—	4
3 ₋₂ → 2 ₋₂	E	145126.386 ^W	31.9	6.86 × 10 ⁻⁶	1.7	7					
3 ₁ → 2 ₁	E	145131.864 ^W	27.1	1.13 × 10 ⁻⁵	2.8	7	} 139(24)	—	—	—	5
3 ₂ → 2 ₂	A	145133.415 ^W	51.6	6.89 × 10 ⁻⁶	1.7	7					
3 ₋₁ → 2 ₋₁	A	146368.328 ^W	28.6	1.13 × 10 ⁻⁵	2.7	7	74(41)	—	—	—	3
9 ₀ → 8 ₁	A	146618.697 ^W	104.4	8.04 × 10 ⁻⁶	2.1	19	92(26)	—	—	—	3
6 ₂ → 7 ₁	A	156127.544 ^W	86.5	6.74 × 10 ⁻⁶	1.0	13	82(30)	—	—	—	3
2 ₁ → 3 ₀	A	156602.395 ^W	21.4	8.93 × 10 ⁻⁶	0.5	5	149(35)	—	—	—	4
7 ₀ → 7 ₋₁	E	156828.517 ^W	70.2	1.88 × 10 ⁻⁵	3.1	15	61(17)	—	—	—	2
6 ₀ → 6 ₋₁	E	157048.617 ^W	54.0	1.96 × 10 ⁻⁵	2.8	13	82(27)	—	—	—	3
1 ₀ → 1 ₋₁	E	157270.832 ^W	7.5	2.21 × 10 ⁻⁵	0.7	3					
3 ₀ → 3 ₋₁	E	157272.338 ^W	19.2	2.15 × 10 ⁻⁵	1.7	7	} 355(53)	—	—	—	8
2 ₀ → 2 ₋₁	E	157276.019 ^W	12.2	2.18 × 10 ⁻⁵	1.2	5					
1 ₁ → 1 ₀	E	165050.175 ^W	15.5	2.35 × 10 ⁻⁵	0.7	3	56(22)	—	—	—	2
2 ₁ → 2 ₀	E	165061.130 ^W	20.1	2.34 × 10 ⁻⁵	1.1	5	232(38)	—	—	—	4
3 ₁ → 3 ₀	E	165099.240 ^W	27.1	2.33 × 10 ⁻⁵	1.6	7	170(28)	—	—	—	6
4 ₁ → 4 ₀	E	165190.475 ^W	36.4	2.32 × 10 ⁻⁵	2.0	9	178(70)	—	—	—	6
5 ₁ → 5 ₀	E	165369.341 ^W	48.0	2.31 × 10 ⁻⁵	2.4	11	127(25)	—	—	—	4
6 ₁ → 6 ₀	E	165678.649 ^W	61.9	2.29 × 10 ⁻⁵	2.8	13	312(31)	—	—	—	6
7 ₁ → 7 ₀	E	166169.098 ^W	78.2	2.28 × 10 ⁻⁵	3.2	15	102(23)	—	—	—	4
3 ₂ → 2 ₁	E	170060.592 ^W	28.3	2.55 × 10 ⁻⁵	1.6	7	275(53)	—	—	—	7
1 ₁ → 2 ₀	A	205791.270 ^F	16.8	6.28 × 10 ⁻⁵	0.9	3	47(16)	10.3(0.4)	2.5(0.7)	18	2
4 ₂ → 3 ₁	E	218440.063 ^F	37.6	4.69 × 10 ⁻⁵	1.7	9	180(10)	10.7(0.1)	1.5(0.1)	113	15
8 ₋₁ → 7 ₀	E	229758.756 ^F	81.2	4.19 × 10 ⁻⁵	2.5	17	110(14)	10.7(0.1)	1.5(0.1)	69	5
5 ₁ → 4 ₁	A	239746.219 ^F	49.1	5.66 × 10 ⁻⁵	4.8	11	74(14)	10.4(0.1)	1.4(0.1)	53	3
5 ₀ → 4 ₀	E	241700.159 ^F	40.0	6.04 × 10 ⁻⁵	5.0	11	251(21)	10.8(0.1)	2.6(0.3)	90	7
5 ₋₁ → 4 ₋₁	E	241767.234 ^F	32.5	5.81 × 10 ⁻⁵	4.8	11	357(33)	10.4(0.2)	1.9(0.1)	224	15

Table B.10. continued.

Transition	Sym.*	Frequency	E_u/k	A_{ul}	S_{ul}	g_u	$\int T_{MB} dv$	v_{LSR}	Δv	T_{MB}	S/N
$(J_{K_a, K_c})_u \rightarrow (J_{K_a, K_c})_l$		[MHz]	[K]	[s^{-1}]			[mK km s^{-1}]	[km s^{-1}]	[km s^{-1}]	[mK]	
$5_0 \rightarrow 4_0$	A	241791.352 ^F	34.8	6.05×10^{-5}	5.0	11	646(43)	10.5(0.2)	2.2(0.2)	273	27
$5_{-4} \rightarrow 4_{-4}$	E	241813.255 ^F	114.8	2.18×10^{-5}	1.8	11	38(13)	10.7(0.2)	1.2(0.6)	28	2
$5_1 \rightarrow 4_1$	E	241879.025 ^F	48.0	5.96×10^{-5}	5.0	11	205(25)	10.5(0.3)	3.3(0.6)	56	7
$5_{-2} \rightarrow 4_{-2}$	E	241904.147 ^F	52.8	5.09×10^{-5}	4.2	11	} 179(21)	10.5(0.1)	2.4(0.3)	67	7
$5_2 \rightarrow 4_2$	E	241904.643 ^F	49.2	5.03×10^{-5}	4.2	11					
$5_{-1} \rightarrow 4_{-1}$	A	243915.788 ^F	49.7	5.97×10^{-5}	4.8	11	72(13)	10.8(0.1)	0.7(0.2)	99	7
$2_1 \rightarrow 1_0$	E	261805.675 ^F	20.1	5.57×10^{-5}	0.7	5	143(10)	10.7(0.1)	1.5(0.1)	89	7
$5_2 \rightarrow 4_1$	E	266838.148 ^F	49.2	7.74×10^{-5}	1.9	11	225(12)	10.7(0.1)	1.7(0.1)	124	10
$9_{-1} \rightarrow 8_0$	E	278304.512 ^F	102.1	7.69×10^{-5}	2.9	19	96(9)	10.7(0.1)	0.9(0.2)	100	10
$6_1 \rightarrow 5_1$	A	287670.767 ^F	62.9	1.01×10^{-4}	5.9	13	80(9)	10.8(0.2)	1.8(0.1)	42	3
$6_{-1} \rightarrow 5_{-1}$	A	292672.889 ^F	63.7	1.06×10^{-4}	5.9	13	82(23)	10.8(0.1)	0.9(0.2)	90	10
$3_0 \rightarrow 2_{-1}$	E	302369.773 ^F	19.2	4.66×10^{-5}	0.5	7	34(14)	10.0(0.1)	0.4(0.2)	84	3
$1_{-1} \rightarrow 1_0$	A	303366.921 ^F	16.9	2.26×10^{-4}	1.0	3	171(14)	10.5(0.1)	1.8(0.1)	89	5
$2_{-1} \rightarrow 2_0$	A	304208.348 ^F	21.6	2.12×10^{-4}	1.6	5	228(14)	10.3(0.1)	1.6(0.1)	134	7
$7_0 \rightarrow 6_0$	E	338124.488 ^F	70.2	1.70×10^{-4}	7.0	15	174(53)	10.5(0.2)	1.6(0.6)	101	3
$7_{-1} \rightarrow 6_{-1}$	E	338344.588 ^F	62.7	1.67×10^{-4}	6.9	15	260(64)	10.7(0.1)	1.5(0.2)	235	11
$7_0 \rightarrow 6_0$	A	338408.698 ^F	65.0	1.70×10^{-4}	7.0	15	440(69)	10.7(0.1)	1.6(0.1)	259	12
$7_3 \rightarrow 6_3$	E	338583.216 ^F	104.8	1.39×10^{-4}	5.8	15	59(20)	11.0(0.1)	0.4(0.1)	133	3
$7_2 \rightarrow 6_2$	E	338721.693 ^F	79.4	1.55×10^{-4}	6.4	15	} 161(22)	10.5(0.1)	1.3(0.1)	117	3
$7_{-2} \rightarrow 6_{-2}$	E	338722.898 ^F	83.0	1.57×10^{-4}	6.5	15					

Notes. Frequencies, E_u/k , A_{ul} , S_{ul} , and g_u from JPL catalogue.

Table B.11. Line parameters of CH₃CHO.

Transition	Sym.*	Frequency	E_u/k	A_{ul}	S_{ul}	g_u	$\int T_{MB} dv$	v_{LSR}	Δv	T_{MB}	S/N
$(J_{K_a, K_c})_u \rightarrow (J_{K_a, K_c})_l$		[MHz]	[K]	[s^{-1}]			[mK km s^{-1}]	[km s^{-1}]	[km s^{-1}]	[mK]	
$5_{1,5} \rightarrow 4_{1,4}$	A	93580.909 ^F	15.7	2.63×10^{-5}	5.2	11	60(6)	10.4(0.1)	2.7(0.3)	21	6
$5_{1,5} \rightarrow 4_{1,4}$	E	93595.235 ^F	15.7	2.63×10^{-5}	5.2	11	51(7)	10.8(0.2)	2.3(0.4)	21	6
$5_{0,5} \rightarrow 4_{0,4}$	E	95947.437 ^F	13.8	2.96×10^{-5}	5.4	11	29(6)	10.7(0.3)	2.0(0.4)	13	3
$5_{0,5} \rightarrow 4_{0,4}$	A	95963.459 ^F	13.8	2.95×10^{-5}	5.4	11	54(13)	10.7(0.2)	2.0(0.5)	25	3
$5_{1,4} \rightarrow 4_{1,3}$	E	98863.314 ^F	16.5	3.10×10^{-5}	5.2	11	79(6)	11.1(0.3)	2.9(0.5)	26	3
$5_{1,4} \rightarrow 4_{1,3}$	A	98900.944 ^F	16.5	3.11×10^{-5}	5.2	11	63(10)	11.1(0.1)	1.6(0.3)	38	7
$6_{1,6} \rightarrow 5_{1,5}$	A	112248.716 ^F	21.1	4.67×10^{-5}	6.3	13	57(10)	10.7(0.2)	2.0(0.3)	27	5
$6_{1,6} \rightarrow 5_{1,5}$	E	112254.508 ^F	21.1	4.67×10^{-5}	6.3	13	46(11)	11.2(0.2)	1.9(0.5)	23	4
$6_{0,6} \rightarrow 5_{0,5}$	E	114940.175 ^F	19.4	5.16×10^{-5}	6.5	13	95(18)	11.0(0.2)	2.2(0.5)	40	4
$6_{0,6} \rightarrow 5_{0,5}$	A	114959.902 ^F	19.4	5.15×10^{-5}	6.5	13	106(15)	10.6(0.1)	2.0(0.3)	49	5
$7_{1,7} \rightarrow 6_{1,6}$	A	130891.821 ^W	27.4	7.54×10^{-5}	7.4	15	} 135(44)	—	—	—	4
$7_{1,7} \rightarrow 6_{1,6}$	E	130892.749 ^W	27.4	7.55×10^{-5}	7.4	15					

Table B.11. continued.

Transition ($J_{K_a, K_c})_u \rightarrow (J_{K_a, K_c})_l$	Sym.*	Frequency [MHz]	E_u/k [K]	A_{ul} [s ⁻¹]	S_{ul}	g_u	$\int T_{MB} dv$ [mK km s ⁻¹]	v_{LSR} [km s ⁻¹]	Δv [km s ⁻¹]	T_{MB} [mK]	S/N
7 _{1,6} → 6 _{1,5}	A	138319.628 ^W	28.8	8.90×10^{-5}	7.4	15	166(62)	—	—	—	3
8 _{1,8} → 7 _{1,7}	E	149505.128 ^W	34.6	1.14×10^{-4}	8.5	17	} 193(96)	—	—	—	2
8 _{1,8} → 7 _{1,7}	A	149507.462 ^W	34.6	1.14×10^{-4}	8.5	17					
8 _{0,8} → 7 _{0,7}	E	152607.614 ^W	33.1	1.23×10^{-4}	8.6	17	184(74)	—	—	—	4
8 _{1,7} → 7 _{1,6}	E	157937.697 ^W	36.4	1.34×10^{-4}	8.5	17	86(21)	—	—	—	4
8 _{1,7} → 7 _{1,6}	A	157974.590 ^W	36.4	1.34×10^{-4}	8.5	17	105(24)	—	—	—	6
9 _{1,9} → 8 _{1,8}	E	168088.618 ^W	42.6	1.64×10^{-4}	9.6	19	} 98(36)	—	—	—	3
9 _{1,9} → 8 _{1,8}	A	168093.444 ^W	42.7	1.64×10^{-4}	9.6	19					
9 _{0,9} → 8 _{0,8}	A	171296.985 ^W	41.3	1.75×10^{-4}	9.7	19	158(92)	—	—	—	2
11 _{1,11} → 10 _{1,10}	E	205161.898 ^F	61.4	3.02×10^{-4}	11.7	23	74(10)	10.6(0.2)	2.4(0.3)	29	4
11 _{1,11} → 10 _{1,10}	A	205170.686 ^{F,B}	61.5	3.01×10^{-4}	11.7	23	—	—	—	—	—
11 _{0,11} → 10 _{0,10}	A	208267.045 ^F	60.4	3.17×10^{-4}	11.8	23	62(9)	10.6(0.1)	1.8(0.3)	33	5
11 _{1,10} → 10 _{1,9}	E	216581.930 ^F	64.8	3.55×10^{-4}	11.7	23	47(10)	10.7(0.2)	1.4(0.5)	32	5
11 _{1,10} → 10 _{1,9}	A	216630.234 ^F	64.8	3.55×10^{-4}	11.7	23	53(7)	10.7(0.1)	1.5(0.2)	33	5
12 _{1,12} → 11 _{1,11}	E	223650.093 ^F	72.2	3.92×10^{-4}	12.8	25	68(9)	10.8(0.1)	1.9(0.3)	34	6
12 _{1,12} → 11 _{1,11}	A	223660.603 ^F	72.2	3.92×10^{-4}	12.8	25	58(11)	10.7(0.2)	2.2(0.5)	24	4
12 _{0,12} → 11 _{0,11}	E	226551.622 ^F	71.3	4.10×10^{-4}	12.9	25	114(6)	10.5(0.3)	2.5(0.5)	43	6
12 _{0,12} → 11 _{0,11}	A	226592.725 ^F	71.3	4.10×10^{-4}	12.9	25	54(15)	11.4(0.1)	1.0(0.4)	50	4
12 _{1,11} → 11 _{1,10}	E	235996.212 ^F	76.1	4.61×10^{-4}	12.8	25	77(23)	10.8(0.3)	2.0(0.8)	36	3
12 _{1,11} → 11 _{1,10}	A	236049.131 ^F	76.1	4.61×10^{-4}	12.8	25	39(15)	10.8(0.2)	1.0(0.5)	38	3
13 _{1,13} → 12 _{1,12}	A	242118.136 ^F	83.8	5.00×10^{-4}	13.9	27	43(17)	10.0(0.5)	2.5(1.3)	16	2
13 _{0,13} → 12 _{0,12}	A	244832.176 ^F	83.1	5.18×10^{-4}	13.9	27	48(10)	11.5(0.1)	1.2(0.3)	39	3
13 _{1,12} → 12 _{1,11}	E	255326.968 ^F	88.4	5.86×10^{-4}	13.9	27	65(13)	10.9(0.2)	2.0(0.5)	30	5
13 _{1,12} → 12 _{1,11}	A	255384.754 ^F	88.4	5.86×10^{-4}	13.9	27	67(10)	10.6(0.1)	1.8(0.3)	34	6
14 _{0,14} → 13 _{0,13}	E	262960.097 ^F	95.7	6.44×10^{-4}	15.0	29	32(7)	10.5(0.2)	1.3(0.3)	23	4
14 _{1,13} → 13 _{1,12}	E	274563.412 ^F	101.5	7.31×10^{-4}	15.0	29	38(11)	10.9(0.2)	1.0(0.3)	35	2
15 _{1,15} → 14 _{1,14}	A	278939.438 ^F	109.7	7.69×10^{-4}	16.1	31	22(7)	10.5(0.2)	1.0(0.4)	23	3
15 _{0,15} → 14 _{0,14}	A	281126.944 ^F	109.2	7.88×10^{-4}	16.1	31	29(11)	10.7(0.3)	1.4(0.5)	19	2

Notes. ^B Blended with CF⁺ 2 → 1. Frequencies, E_u/k , A_{ul} , S_{ul} , and g_u from JPL catalogue.